Mutations in the "Dynein Regulatory Complex" Alter the ATP-insensitive Binding Sites for Inner Arm Dyneins in *Chlamydomonas* Axonemes

Gianni Piperno, Kara Mead, Michel LeDizet, and Alessandra Moscatelli

Department of Cell Biology and Anatomy, Mount Sinai School of Medicine, New York 10029

Abstract. To understand mechanisms of regulation of dynein activity along and around the axoneme we further characterized the "dynein regulatory complex" (*drc*). The lack of some axonemal proteins, which together are referred to as *drc*, causes the suppression of flagellar paralysis of radial spoke and central pair mutants. The *drc* is also an adapter involved in the ATP-insensitive binding of I2 and I3 inner dynein arms to doublet microtubules. Evidence supporting these conclusions was obtained through analyses of five *drc* mutants: *pf2*, *pf3*, $sup_{pf}3$, $sup_{pf}4$, and $sup_{pf}5$. Axonemes from *drc* mutants lack part of I2 and I3 inner dynein arms as well as subsets of seven *drc* components (apparent molecular weight from 29,000 to 192,000). In the absence of ATP-Mg, dynein-depleted axonemes from the same mutants bind I2 and I3 inner arms at both ATP-sensitive and -insensitive sites. At ATP-insensitive sites, they bind I2 and I3 inner arms to an extent that depends on the *drc* defect. This evidence suggested to us that the *drc* forms one binding site for the I2 and I3 inner arms on the A part of doublet microtubules.

VARIOUS types of dynein arms (13) together cause axonemal microtubules to slide relative to one another and ultimately generate the oscillatory movements of the axonemes. Therefore, axoneme bending results from the coordinated regulation of dynein activities along and around the axoneme structure. Understanding that regulation and, in particular, understanding mechanisms of local activation and/or inactivation of dynein arms would be major achievements in the study of axonemal motility. Towards these goals, we intend to further characterize the "dynein regulatory complex" (*drc*)[1] (12) a complex that may modify (in wild-type strains) or inhibit (in radial spokes and central complex mutants) (3, 7) the dynein-mediated sliding of doublet microtubules.

The *drc* is composed of six axonemal proteins that in subsets are lacking from the axoneme of nine mutants, representing five loci of the *Chlamydomonas* genome (7, 12). Some mutations of the *drc* were isolated as motility mutants, others as second-site suppressors that release the paralysis of flagella of radial spoke mutants without repairing the original radial spoke defects (7, 12). The same mutations in a wild-type background cause inefficient axonemal beating (2) and decrease the number of I2 and I3 inner dynein arms bound to doublet microtubules (12).

Two observations suggested that the *drc* may be a structure linking I2 and I3 inner arms to neighboring structures such as the A part of doublet microtubules or the outer dynein arms. First, the analysis of recombinant strains carrying inner arm and *drc* mutations indicated that I2 inner arms interact with the *drc* (12). Second, analyses of electron micrographs showed that a structure located between I2 and I3 inner arms and the outer dynein arms is missing in the *drc* mutant *pf2* (10). Components of the *drc*, then, may form binding sites for inner dynein arms that are located on the A part of doublet microtubules. This hypothesis will be tested by experiments described in this article.

We performed a new characterization of the *drc* mutants *pf2*, *pf3*, $sup_{pf}3$, $sup_{pf}4$, and $sup_{pf}5$ through the following steps. First, we determined whether all *drc* mutants suppress the paralysis of both radial spoke and central pair mutants. Second, we determined whether the I1 inner arms, similarly to the I2 and I3 inner arms, are defective in these mutants. Then, we determined whether, in vitro, the *drc* affects the binding of inner arms. Finally, we identified one new component of the *drc* and tested the hypothesis that *drc* components are defective gene products of specific *drc* mutants.

These analyses identified the *drc* as a large structure (apparent molecular weight at least 500,000) that has the following properties: (*a*) it suppresses the paralysis of both radial spoke and central pair mutants; (*b*) it affects the binding of all types of inner arms; (*c*) it forms ATP-insensitive binding sites for I2 and I3 inner dynein arms in vitro; and (*d*) it is

Address all correspondence to G. Piperno, Department of Cell Biology and Anatomy, Mount Sinai School of Medicine, Box 1007, One Gustave L. Levy Place, New York, NY 10029.

Dr. Moscatelli's present address is Dipartimento di Biologia Ambientale, Universita' degli Studi di Siena, 53100 Siena, Italy.

1. *Abbreviations used in this paper*: *drc*, dynein regulatory complex; LISB, low ionic strength buffer.

tightly bound to the microtubule lattice. The *drc*, then, is the first example of a microtubule-associated structure that mediates the interactions between the ATP-insensitive binding domains of dyneins and the microtubule lattice. Further studies of the *drc* function can be approached by genetics because at least two *drc* components are putative defective gene products of *drc* mutations.

Materials and Methods

Strains and Culture of Chlamydomonas Cells

Cell culture and labeling with [^{35}S]sulfuric acid were performed in solid medium (13).

Strains of *drc* mutants were crossed once to the wild-type strain 137 and tetrads of daughter cells were obtained by standard methods (4). Each mutant could be distinguished from the wild-type strain because mutant cell bodies move less efficiently. Although detailed analysis of the motion of cells from each strain was not performed, the motility phenotype of each *drc* mutant qualitatively was distinguishable from that of the wild-type strain by optical microscopy. Mutants derived from the cross to the wild-type strain were characterized further throughout this study. The lack or defect of *drc* components within the axonemes of each mutant was determined by one- and two-dimensional electrophoresis of axonemal proteins. This analysis confirmed the existence of a deficiency of different subsets of *drc* components in each mutant (Table III) as observed by Huang et al. (7) and Piperno et al. (12).

Recombinant strains between each of the *drc* mutant and the central complex mutant *pf*15 or *pf*18 (1) or the radial spoke mutant *pf*1 or *pf*14 (6) were obtained from nonparental ditype tetrads. Phenotypic analysis of recombinants was performed by optical microscopy on cells that were grown for 1 d at 25°C in medium containing sodium acetate as described by Sager and Granick (16). Suppression of flagellar paralysis was scored if paralysis or erratic movement of flagella of radial spoke or central pair mutants was changed to regular beating of flagella of the recombinants.

Recombinant strains between the mutant *pf*28 (11) and each of the *drc* mutants were obtained from nonparental ditype tetrads with the exception of *pf*2*pf*28 that was obtained from a tetratype tetrad. The majority of *pf*2*pf*28 cells did not have flagella. The recombinants *pf*3*pf*28 and sup_{pf}5*pf*28 had short and paralyzed flagella. The cell bodies of sup_{pf}3*pf*28 did not move but had a minority of flagella beating. The cell bodies of sup_{pf}4*pf*28 were all propelled by the movement of flagella.

Dikaryon rescue analyses were performed as described before (9). Gametes were grown for 8 d on solid minimal medium. Rescue of *drc* components did not require flagellar regeneration from the dikaryons. Mutant cells were labeled by growth on ^{35}S-containing medium. Fusion between ^{35}S-labeled mutant and unlabeled wild-type gametes was carried out in the presence of anisomycin to inhibit protein synthesis in the dikaryon. Putative restoration of function within mutant flagella of the dikaryon was correlated with the assembly of ^{35}S-labeled mutant and unlabeled wild-type polypeptides in mutant axonemes. In the case of the mutant gene product only an unlabeled wild-type polypeptide could be incorporated. Therefore, the component that is lacking from the maps of ^{35}S-labeled axonemal components of mutant-wild-type dikaryons was identified as the putative defective gene product of the mutant.

Binding of Inner Arm Heavy Chains to Dynein-depleted Axonemes

We have modified the procedure of Smith and Sale (17) as follows. Axonemes were prepared by the dibucain method (18) and collected by centrifugation at 10,000 rpm for 15 min in a SS34 rotor (Sorvall, Du Pont Co., Newton, CT). Then, they were resuspended at concentrations close to 2 mg/ml in 50 mM NaCl, 0.5 mM EDTA, 10 mM Hepes, pH 7.4, in the presence of pepstatin A and leupeptin (referred to as low ionic strength buffer [LISB]). In order to extract the dyneins, half of each axoneme suspension was exposed to 0.55 M NaCl, 4 mM $MgCl_2$, 1 mM ATP, 10 mM Hepes, pH 7.4, and sedimented at 9,000 rpm for 5 min at 4°C in a Eppendorf 5402 centrifuge (Brinkmann Instruments Inc., Westbury, NY). Pellets of dynein-depleted axonemes were washed once with LISB and then resuspended in the same solution at a protein concentration close to 2 mg/ml. An aliquot of the dynein-containing salt extract from ^{35}S-labeled *pf*28 axonemes was recovered (0.3–0.5 ml containing 0.3–0.5 mg/ml of protein, specific radioactivity 50,000 cpm/μg), dialyzed in a membrane tubing (12,000–14,000-mol wt cutoff; Spectra/por, Los Angeles, CA) for 1 h against ice-cooled LISB and centrifuged at 14,000 rpm for 5 min at 4°C in the Eppendorf centrifuge to sediment any aggregate of dynein arms that could be formed during the dialysis. Extracts contained 90% of the I1 and 80% of the I2 and I3 inner dynein arm heavy chains originally present in the *pf*28 axonemes. Dynein-containing extracts were then mixed with dynein-depleted or nonextracted axonemes at 0.5:1, 1.5:1, and 2:1 protein ratios. Each sample was processed in double. Incubation of suspensions was performed at room temperature for 15 min. Samples were then centrifuged at 14,000 rpm for 5 min at 4°C in the Eppendorf centrifuge in the presence or absence of 1 mM ATP, 4 mM $MgCl_2$. Pellets were washed once with LISB solution and then solubilized in 1% SDS, 1% β-mercaptoethanol.

Protein samples, ~6 μg, were divided in half and subjected to electrophoresis: half on a 3.6–5% and the other half on a 4–11% polyacrylamide gel. Amounts of bound ^{35}S-labeled dynein heavy chains were determined by the PhosphorImager analysis of the 3.6–5% gels, whereas amounts of Coomassie blue–stained tubulin subunits were determined by densitometric analysis of the 4–11% gels. Determinations of tubulin amounts were performed to confirm that each lane of the gel contained equal amounts of protein. Radioactivity and optical density values, as measured by the PhosphorImager or the optical densitometer, were in the linear range of response of the instruments.

Amounts of heavy chains bound to nonextracted axonemes (representing binding to sites other than dynein binding sites, also referred to as nonspecific binding) were subtracted from amounts of inner arm heavy chains bound to dynein-depleted axonemes. The second were 3 to 11 times higher then the first, depending on the experiment. The same subtraction was performed for the samples processed in the presence of ATP. In this case both nonextracted and extracted axonemes were processed in the presence of ATP, although amounts of heavy chains bound to nonextracted axonemes were not sensitive to the presence of ATP.

Amounts of I1, I2, and I3 inner arm heavy chains bound to axonemes in some cases were normalized for the amounts of tubulin. This correction was introduced if gel lanes did not contain equal amounts of protein, in spite of the fact that we attempted to analyze exactly 3 μg of protein. Amounts of I2 and I3 inner arm heavy chains bound to 3 μg of dynein-depleted axonemes were 15–60% of the amounts of the same heavy chains that were present in 3 μg of ^{35}S-labeled *pf*28 axonemes.

Other Procedures

Dialysis of dynein-depleted wild-type axonemes was performed at a protein concentration of 1 mg/ml for 2 h, at 0°C, against a solution of 0.5 mM NaCl, 0.5 mM EDTA, 1 mM Hepes, pH 7.4.

One-dimensional resolution of dynein heavy chains or tubulin subunits, two-dimensional resolution of axonemal components (12), determination of flagellar length (13) were performed as we previously described. Resolution of basic proteins by two-dimensional electrophoresis was achieved by nonequilibrium pH gradient electrophoresis run for 14 h at 1.4 mA, other conditions were as in reference 12.

Results

Mutations in the drc Suppress Flagellar Paralysis of Both Central Complex and Radial Spoke Mutants

Following the observation of Huang et al. (7) that mutants, *pf*2, *pf*3, sup_{pf}3, and sup_{pf}4 suppress the paralysis of radial spoke mutants and our observation that the mutation sup_{pf}5 suppresses flagellar paralysis of both central complex and radial spoke mutants (12) we intended to determine whether the other *drc* mutants, *pf*2, *pf*3, sup_{pf}3, and sup_{pf}4, are similar to sup_{pf}5 for their suppressor effect toward the paralysis of central complex mutants. We isolated recombinant strains between each of the *drc* mutant *pf*2, *pf*3, sup_{pf}3, and sup_{pf}4 and the central complex mutants *pf*15 and *pf*18 (1). We also isolated recombinants between the same *drc* mutants and the radial spoke mutants *pf*1 and *pf*14 (6).

We observed each recombinant by optical microscopy and found that paralysis or erratic movement of flagella in central

complex and radial spoke mutants was changed into regular beating in each recombinant strain. However, the cell body of the recombinants was not propelled by the movement of flagella. From this evidence we concluded that the *drc* mutants *pf*2, *pf*3, sup_{pf}3, and sup_{pf}4 suppress the paralysis of central complex as well as radial spoke mutants, similarly to the *drc* mutant sup_{pf}5 and other suppressors of paralysis such as sup_{pf}1 and sup_{pf}2 (7).

Flagella of drc Mutants Are Deficient in All Types of Inner Dynein Arms

To address the question of whether the I1 inner dynein arms are deficient in the *drc* mutants, we eliminated the outer dynein arms from their axonemes by introducing the mutation *pf*28 (11). Our past analyses of flagellar proteins from *drc* mutants determined that I2 and I3 inner dynein arm heavy chains were present in reduced amounts in these mutants (12). However, the same analyses could not determine whether I1 inner arm heavy chains were also defective because these heavy chains have the same electrophoretic mobility as the outer arm heavy chains.

We isolated recombinant strains *pf2pf28*, *pf3pf28*, sup_{pf}*3pf28*, sup_{pf}*4pf28*, and sup_{pf}*5pf28* and analyzed inner arm heavy chains from *pf3pf28*, sup_{pf}*3pf28*, sup_{pf}*4pf28*, and sup_{pf}*5pf28* by gel electrophoresis of ^{35}S-labeled flagellar proteins. The recombinant *pf2pf28* could not be analyzed because the majority of the cells did not have flagella and the rest had very short stubs. We analyzed flagella and not axonemes to avoid losses of dynein arms that could occur during the isolation of the axonemes. Moreover, we adopted the mass of tubulin subunits as an internal standard of each sample in order to normalize the data. Therefore, we performed qualitative and quantitative analyses of inner arms heavy chains by electrophoretic conditions that resolved heavy chains and tubulin subunits in the same slab gel.

The electrophoretogram of ^{35}S-labeled proteins from flagella of a wild-type strain is in Fig. 1. The major flagellar membrane protein, the dynein heavy chains and the tubulin subunits were resolved in spite of their large difference of apparent molecular weight (14).

Portions of electrophoretograms resolving the inner arms heavy chains from *pf*28 and recombinants *pf3pf28*, sup_{pf}*3pf28*, sup_{pf}*4pf28*, and sup_{pf}*5pf28* are shown in Fig. 2. They were obtained from Experiment 1 described in Table I. Flagella of the recombinant *pf3pf28*, sup_{pf}*3pf28*, and sup_{pf}*5pf28* lack the 3′ inner arm heavy chain and are shorter than 6 μm (Table I) similarly to some inner arm mutants (13).

Results of quantitative analyses of inner arm heavy chains from recombinants *pf3pf28*, sup_{pf}*3pf28*, sup_{pf}*4pf28*, and sup_{pf}*5pf28* and the mutant *pf28* are reported in Table I. Calculations were performed as follows: (*a*) radioactivity backgrounds were subtracted from the radioactivity of each inner arm heavy chain; and (*b*) ratios of inner arm heavy chains to tubulin radioactivities were expressed as percentages of the ratio that was obtained for the mutant *pf*28. Quantities of I1, as well as those of I2 and I3 inner arm heavy chains, are lower in recombinants than in *pf28*. Recombinant sup_{pf}*5pf28* is the most defective, whereas sup_{pf}*4pf28* is the least defective, in both inner arm content and flagellar length. Therefore, some *drc* defects may affect the binding of all types of inner arms to the axonemes, if a reduction of flagellar length does not affect the inner arm content of the recombinants.

To determine whether the reduction of all inner arm heavy chains depends on flagellar length we prepared 3-μm-long flagella of *pf28* by separation and regeneration of flagella from that mutant. Following this preparation we measured the content of inner arms present in the 3-μm-long flagella. We found that short or long *pf28* flagella contain approximately the same amount of inner arm heavy chains relatively to the amount of tubulin (Table I). These results indicated that a reduction of inner arm concentration is correlated with a *drc* defect and not with a reduction of flagellar length. However, the last experiment could be meaningless, if equilibrium of assembly of inner arms in regenerating flagella of *pf*28 are different from those in stable flagella of recombinant strains.

Additional experiments performed with flagellar proteins from the *drc* mutants *pf*2, *pf*3, sup_{pf}*3*, sup_{pf}*4*, and sup_{pf}*5* indicated that outer arm heavy chains are not significantly reduced in these mutants. Moreover, experiments performed

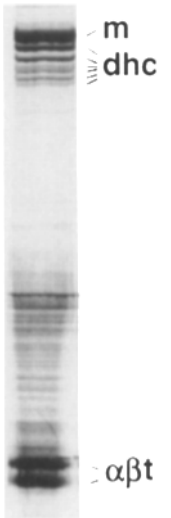

Figure 1. Autoradiogram of ^{35}S-labeled flagellar polypeptides from a wild-type strain. Polypeptides were resolved by a discontinuous gel consisting of a 13% polyacrylamide section topped by a 3.6–5% polyacrylamide gradient gel. Autoradiogram was obtained by the PhosphorImager. Bands referred to as *m*, *dhc*, and *αβt* are a membrane protein, outer and inner dynein arm heavy chains and α and β tubulin subunits, respectively.

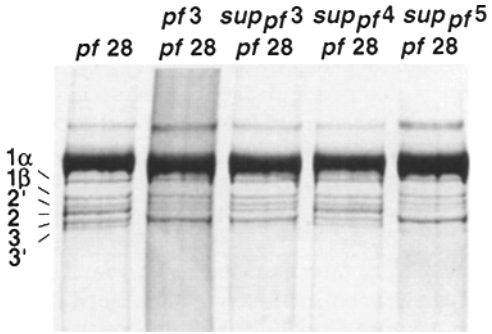

Figure 2. Autoradiogram of ^{35}S-labeled flagellar polypeptides from the mutant *pf*28 and recombinants *pf3pf28*, sup_{pf}*3pf28*, sup_{pf}*4pf28*, and sup_{pf}*5pf28*. A portion of the original autoradiogram resolving polypeptides in the 500,000-400,000 apparent molecular weight range is shown. Equal amounts of radioactivity were analyzed in each lane under conditions described in the legend of Fig. 1. Couples of bands (referred to as *1α* and *1β*, *2′* and *2*, and *3* and *3′*) are heavy chains of the inner arms I1, I2, and I3, respectively.

*Table I. Quantitative Analyses of the Content of Inner Arm Heavy Chains in Flagella**

	*pf*28		*pf*2*pf*28	*pf*3*pf*28	sup_{pf}3*pf*28	sup_{pf}4*pf*28	sup_{pf}5*pf*28
	a‡	*b*‡					
Experiment 1							
I1 inner arms	100	102	ND§	55	71	87	41
I2&I3 inner arms	100	93	ND	49	48	69	41
Flagellar length (μm)	13.0(0.9)	3.0(0.6)	<1	4.5(0.9)	6.4(2.2)	12.7(1.3)	2.4(0.7)
Experiment 2							
I1 inner arm	100	102	ND	71	57	77	29
I2&I3 inner arms	100	92	ND	65	43	84	41
Flagellar length (μm)	10.3(1.0)	3.6(0.5)		3.4(0.6)	3.2(0.6)	8.5(1.8)	2.7(0.8)

* Standard deviations of radioactivity values obtained by the PhosphorImager were lower than 8%. Numbers are percentages of values that were obtained for full-length flagella (*a*) of the mutant *pf*28. Number in parenthesis are standard deviations of length determinations.
‡ *a*, full-length flagella; *b*, regenerating flagella.
§ ND, not determined. The majority of *pf*2*pf*28 cells does not have flagella.

with the radial spoke mutant *pf*14 indicated that the lack of radial spokes does not affect the assembly of I2 and I3 inner arm heavy chains (not shown).

In summary, the lack of a subset of *drc* components in each recombinant may cause the reduction in concentration of all types of inner arms within flagella. Assuming that the reduction of inner arm concentration is a direct consequence of a *drc* defect, then, some *drc* components may form binding sites for inner arms on doublet microtubules. This hypothesis was tested by experiments described in the following sections.

Inner Arm Heavy Chains Bind to Dynein-depleted Axonemes at ATP-sensitive and -insensitive Sites

Our previous analyses of *drc* mutants indicated that at least I2 inner arms interact with the *drc* (12). However, we did not test the following possibilities: (*a*) the *drc* forms a binding site for the inner arms; (*b*) the *drc* modifies the inner arm subunits to make them competent to bind other structures; and (*c*) flagellar matrix proteins are necessary for the inner arm binding to doublet microtubules. To establish that the *drc* components are responsible for the formation of inner arm binding sites, we performed an assay that allowed us to measure the amount of inner arm heavy chains bound in vitro to axonemes depleted of dynein and matrix proteins.

The binding assay is based on the evidence, which will be described later, showing that the *drc* is not extracted from the axoneme under conditions that extract inner arm heavy chains. The assay is described in detail in Materials and Methods and was performed as follows. First, all types of outer and inner arm heavy chains were extracted from unlabeled axonemes of wild-type and *drc* mutants. Second, an ^{35}S-labeled extract containing all inner arm but not outer arm heavy chains was mixed with a suspension of extracted axonemes from wild-type or *drc* mutants. Following an incubation the axonemes were pelleted, washed, and solubilized by SDS. Finally, ^{35}S-labeled axonemal components were analyzed qualitatively and quantitatively by gel electrophoresis.

Nonextracted axonemes from wild-type and *drc* mutants were processed in parallel to extracted axonemes from the same strains to measure the level of nonspecific binding of inner arm heavy chains. Samples of extracted and nonextracted axonemes from wild-type or *drc* mutants were exposed to the same ^{35}S-labeled extract containing inner arm heavy chains. Both samples of extracted and nonextracted axonemes were processed in the same conditions.

Following an incubation with inner arm heavy chains at a protein ratio 2:1, nonextracted and extracted wild-type axonemes generated silver-stained electrophoretic patterns of dynein heavy chains that respectively are similar to the electrophoretic patterns of heavy chains from wild-type and outer arm-less axonemes (Fig. 3 *a*). Outer arm heavy chains are undetectable in the sample of extracted wild-type axonemes. The corresponding autoradiograms obtained by the PhosphorImager revealed that the ^{35}S-labeled inner arm heavy chains bound much more to extracted axonemes than to nonextracted axonemes (Fig. 3 *b*). Moreover, nearly the totality (93%) of ^{35}S-labeled inner arm heavy chains bound to extracted axonemes were re-extracted in the presence of 0.55 M NaCl, 1 mM ATP, 4 mM $MgCl_2$ (not shown). Therefore, the evidence indicates that axonemes exposed to high concentration of NaCl carry a higher number of inner arm binding sites than nonextracted axonemes and bind inner arms in a reversible fashion.

Quantitative and qualitative analyses of Fig. 3 *b* by the

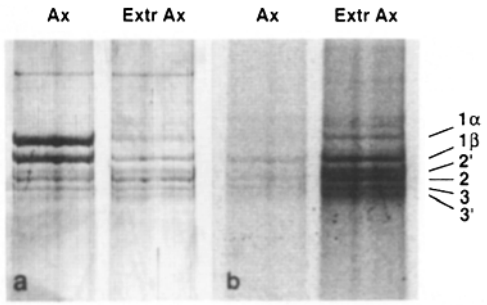

Figure 3. Electrophoretograms of dynein heavy chains as obtained by electrophoresis in a 3.6–5% polyacrylamide gel. Portions of electrophoretograms resolving polypeptides in the 500,000–400,000 apparent molecular weight range are shown. (*a*) Electrophoretograms of polypeptides from unlabeled wild-type axonemes that were exposed to a solution containing ^{35}S-labeled inner dynein arms from the mutant *pf*28, before, first lane, and after, second lane, extraction of dynein heavy chains. Gel was stained by silver. (*b*) Autoradiogram of the gel portion shown in *a*. Couples of bands (referred to as *1α* and *1β*, *2'* and *2*, and *3* and *3'* are heavy chains of the inner arms I1, I2, and I3, respectively. Autoradiogram was obtained by the PhosphorImager.

PhosphorImager indicated that I2 and I3 inner arm heavy chains together bound to extracted axonemes 7.7 times more than to nonextracted axonemes and were retained in stoichiometric amounts. However, the I1 inner arm heavy chains behaved differently than I2 and I3 heavy chains because they bound to extracted axonemes only 4.0 times more than nonextracted axoneme. Furthermore, the 1α heavy chain was retained in an amount that is 20% of the amount of the 1β heavy chain (the ratio of 1α and 1β heavy chains is 1:1 in vivo and in the ^{35}S-labeled dynein-containing extract [not shown]).

The capacity of binding of extracted axonemes is saturated at a protein ratio of 1.5:1 between ^{35}S-labeled extract and extracted axonemes for all types of inner arm heavy chains (Fig. 4).

To determine whether the inner arm heavy chains bind through their ATP-insensitive portion (as they do in vivo on the A part of doublet microtubules) and/or through their ATP-sensitive portion (as they do in vivo on the B part of doublet microtubules) we measured the amounts of bound inner arm heavy chains that remain on extracted axonemes after an exposure to 1 mM ATP and 4 mM $MgCl_2$. The amount of each inner arm heavy chain was reduced to ~60% of the amount bound in the absence of ATP (not shown). Saturation of binding was obtained at a protein ratio of 1.5:1 between ^{35}S-labeled extract and extracted axonemes also in the presence of ATP.

In summary, the binding of stoichiometric amounts of I2 and I3 inner arm heavy chains is reversible, saturable, and mostly occurs at ATP-insensitive sites. Moreover, this binding does not require the presence of matrix proteins or ATP because it occurs on extracted axonemes and in the absence of ATP. This evidence indicates that I2 and I3 inner arm heavy chains can be used to determine whether specific axonemal components form inner arm binding sites. In contrast, the I1 inner arm heavy chains are not suitable for the same purpose because a large portion of I1 inner arms is dissociated irreversibly during the experiment.

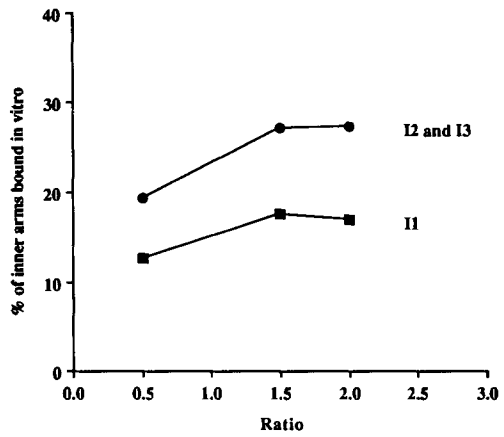

Figure 4. Diagram representing the amounts of inner arm heavy chains bound to dynein-depleted axonemes as function of the ratio between the amounts of ^{35}S-labeled dynein extract from the mutant pf 28 and unlabeled dynein-depleted axonemes from a wild-type strain. The amounts of inner arm heavy chains bound to dynein-depleted axonemes are expressed as percentage of the homologous heavy chains bound in vivo in *pf*28 axonemes. (●—●), curve representing the I2 and I3 heavy chains. (■—■), curve representing the I1 heavy chains.

Binding of I2 and I3 Inner Arms to ATP-insensitive Sites Is Lower in drc Mutants Than in Wild-type Axonemes

To determine whether some *drc* components form a binding site for the inner arms we measured the amount of ^{35}S-labeled inner arm heavy chains that remain bound to unlabeled extracted axonemes of each of the *drc* mutants at the protein ratio 2:1 between inner arm and extracted axoneme. Inner arm heavy chains first were bound to unlabeled extracted axonemes in the absence of ATP-Mg, and then were exposed to the presence of ATP-Mg. We limited our analysis to the I2 and I3 inner arm heavy chains bound to ATP-insensitive sites because the *drc* is located on the A part of the doublet microtubules, the site where the inner arm base is connected in an ATP-insensitive fashion.

The amounts of I2 and I3 inner arm heavy chains bound to extracted axonemes of a wild-type strain were higher than those bound to extracted axonemes of *pf*2, *pf*3, and sup_{pf}5 and similar to those bound to extracted axonemes of sup_{pf}4 and sup_{pf}3 (Table II).

This evidence indicates that the number and/or the affinity of I2 and I3 inner arm binding sites in axonemes of a subset of *drc* mutants is lower than in wild-type axonemes. The decrease of inner arm binding to extracted axonemes of *drc* mutants is correlated to the extent of the *drc* defect, which is more severe in *pf*2, *pf*3, and sup_{pf}5 (Table III). Therefore, the absence of some *drc* components in *pf*2, *pf*3, and sup_{pf}5 decreases the number of inner arm binding sites. Alternatively, the absence of these *drc* components decreases the affinity of a subset of the inner arm binding sites. In both cases, a subset of *drc* components, missing in *pf*2, *pf*3, and sup_{pf}5, is involved in the formation of I2 and I3 inner arm binding sites in the A part of doublet microtubules.

The drc Is As Insoluble As Radial Spoke Stalks and As Large As a Dynein Heavy Chain

A necessary condition to evaluate the *drc*'s competence to bind inner arm heavy chains is that the *drc* itself remains bound to doublet microtubules during extraction and rebinding of the inner arms. To determine whether the *drc* remains insoluble after exposure to 0.6 M or 0.5 mM NaCl (ionic conditions that are higher and lower, respectively, than those adopted for extraction and rebinding of inner arms) we analyzed the molecular composition of wild-type axonemes that were exposed to these conditions. Polypeptides components of extracted axonemes were resolved by two-dimensional gel electrophoresis and compared to untreated axonemes, Fig. 5.

*Table II. Quantitative Analyses of the I2 and I3 Inner Arm Heavy Chains Bound in Vitro to Extracted Axonemes**

	Wild-type	*pf*2	*pf*3	sup_{pf}3	sup_{pf}4	sup_{pf}5
Experiment 1	100	46	36	86	100	29
Experiment 2	100	69	58	93	97	34

* Standard deviations of radioactivity values obtained by the PhosphorImager were lower than 8%. The amount of inner arms heavy chains bound to *drc* mutants is expressed as a percentage of the inner arm heavy chains bound to wild-type axonemes.

Table III. Characteristics of drc Components

Component	$M_r \times 10^{-3}$*	Lacking in‡	Putative gene product of
drc 1	83	*pf*3, sup_{pf}5	*pf*3
drc 2	70	*pf*3, sup_{pf}5	Unknown
drc 3	62	*pf*2, sup_{pf}3	Unknown
drc 4	55	*pf*2, sup_{pf}3	Unknown
drc 5	40	*pf*2, *pf*3, sup_{pf}3, sup_{pf}4, sup_{pf}5	sup_{pf}4
drc 6	29	*pf*2, *pf*3, sup_{pf}3, sup_{pf}4, sup_{pf}5	Unknown
drc 7	192	*pf*2	Unknown

* Estimates of apparent molecular weights of *drc* components were obtained by comparing molecular weight standards to *drc* components that were partially purified by FPLC chromatography, then identified by two-dimensional gel electrophoresis and finally isolated by one dimensional gel electrophoresis (Michel Le Dizet, unpublished results). Previous estimates of molecular weights were calculated from two-dimensional maps of polypeptides (7).

‡ The *drc* components 3, 5 and 6 are reduced in amount but not lacking in the mutant sup_{pf}3.

Each of the *drc* components (Fig. 5, *a* and *b*, *arrowheads*) is present in extracted axonemes and is as insoluble as a subset of components of radial spoke stalks (Fig. 5 *b*, *empty arrowheads*). In contrast, a number of dynein components were extracted (Fig. 5 *a*, *lines*).

The resolution of axonemal components by the two-dimensional electrophoresis shown in Fig. 5 is limited to polypeptides of apparent molecular weight approximately <180,000 and isoelectric point comprised between 7.5 and 4. To determine whether the *drc* is composed of polypeptides not resolved under these conditions we compared axonemal components from *drc* mutants and wild-type strains by a variety of procedures, including two-dimensional electrophoresis of basic proteins and one-dimensional electrophoresis of large polypeptides (apparent molecular weight above 180,000).

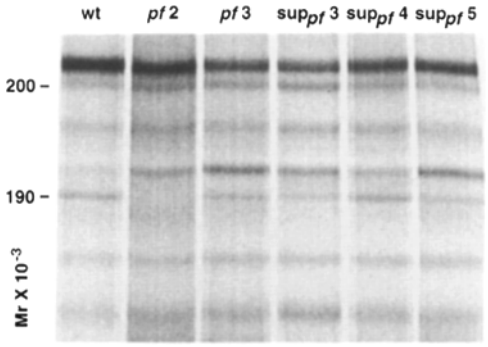

Figure 6. Electrophoretogram of axonemal polypeptides that were resolved by a 5% polyacrylamide gel. The position of molecular weight standards is indicated on the left side. Names of strains under analysis are indicated above each lane.

We were able to observe all the deficiencies in axonemal polypeptides reported before for the mutants *pf*2, *pf*3, sup_{pf}3, and sup_{pf}4 (7). Moreover, we identified a new *drc* component. Fig. 6 shows that an axonemal component of apparent molecular weight 192,000 is missing from the axonemes of the mutant *pf*2 but not from axonemes of other *drc* mutants. The same polypeptide in wild-type axonemes is as insoluble as other *drc* components (not shown). Therefore, it can be regarded as a *drc* component and will be referred to as component 7 (Table III).

The *drc* component 7 is the heaviest. Together with all other *drc* components it may form a complex of at least 530,000 apparent molecular weight and therefore a structure that is as large as a dynein heavy chain or more.

Some of the drc Components Are Putative Defective Gene Products

The identification of a function of each *drc* component will require additional in vivo studies to be performed by approaches of genetics and molecular genetics. As preliminary approach to that development we intended to determine

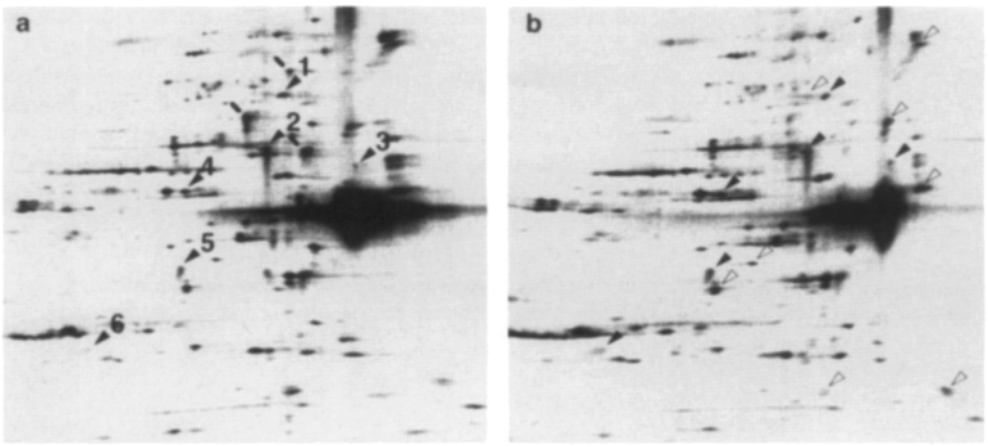

Figure 5. Autoradiograms of ^{35}S-labeled axonemal polypeptides that were resolved by two-dimensional electrophoresis. Only portions of the original maps resolving polypeptides in the 130,000–15,000 molecular weight range are shown. The gels are oriented with the basic polypeptides on the left. Single or double spots are indicated by arrow heads and numbers or lines. They were identified by their position in the maps as *drc* components (*filled arrowheads*), radial spoke stalk components (*empty arrowheads*), and dynein components (*lines*). (*a*) Polypeptides of untreated axonemes. (*b*) Polypeptides of axonemes that subsequently were exposed to solutions of high and low ionic strength under conditions described in Material and Methods.

whether any of the *drc* components is a gene product of a *drc* mutant. Dikaryon rescue analysis of the mutants $sup_{pf}3$ and $sup_{pf}4$ was performed before (7). That analysis identified as putative defective gene products *drc* components 4 and 5, respectively. Our analysis confirmed only the identification of the putative defective gene product of $sup_{pf}4$.

We analyzed the *drc* components by the dikaryon rescue procedure and found that *drc* components 1 and 5 are putative defective gene products of the mutants *pf*3 and $sup_{pf}4$, respectively (Table III). None of the *drc* components appeared to be $SUP_{pf}5$ product. Surprisingly, *drc* component 4 appeared to be gene product of both $sup_{pf}3$ and *pf*2. The study of *pf*2-wild-type dikaryons was performed by both one- and two-dimensional gel electrophoresis of axonemal proteins to include *drc* component 7 in the analysis (not shown).

Two-dimensional maps of ^{35}S-labeled axonemal polypeptides from $sup_{pf}5$-wild-type and *pf*3-wild-type dikaryons are shown as examples of results obtained by the dikaryon rescue procedure. The map of axonemal components from $sup_{pf}5$-wild-type dikaryon (Fig. 7 *a*), is indistinguishable from that of a wild-type strain (compare with Fig. 5 *a*), whereas, the map of axonemal components from *pf*3-wild-type dikaryons (Fig. 7 *b*) is lacking *drc* component 1, the putative defective gene product of *pf*3.

Discussion

The Mechanism of Suppression of Flagellar Paralysis

Our conclusion that the *drc* mutants *pf*2, *pf*3, $sup_{pf}3$, and $sup_{pf}4$ suppress the paralysis of flagella of central complex as well as radial spoke mutants is in contrast with the statement that these mutants do not suppress the paralysis of flagella of central complex mutants (7). The origin of this discrepancy is unknown and may derive from conditions for cell growth before the phenotypic analysis and/or criteria to score suppression.

Suppression of flagellar paralysis in recombinants carrying one *drc* mutation and one central complex or radial spoke mutation is caused by either gaps within the inner arm row (as they occur in *pf*2, *pf*3, $sup_{pf}3$, and $sup_{pf}5$ flagella [12]) or defective control of inner arm activity (this may be caused by the $sup_{pf}4$ mutation, as discussed below). In both cases the cause of suppression is a defect of a dynein arm. The same occurrence was observed also in the suppressors $sup_{pf}1$ (7) and *pf*9-2 (15), which are defective for the β-chain of the outer arms and I1 inner arms, respectively. Therefore, an inhibition of flagellar movement may derive from an inhibition of dynein functions that occurs at different points of the dynein structure.

The inhibition can be bypassed if an axonemal component is missing. This axonemal component can be a dynein arm or part of a subunit of a dynein arm that is the site where the inhibition occurs. If this hypothesis is correct we should be able to find that also the mutant $sup_{pf}2$ is a dynein arm mutant. A molecular phenotype of the mutant $sup_{pf}2$ is unknown, although the mutant $sup_{pf}2$ is a suppressor of flagellar paralysis of central complex and radial spoke mutants (7) like nearly all other suppressors of paralysis that are known (with the exception of the mutant *pf*9-2; reference 15).

Flagella of drc Mutants Lack Some of the Inner Arms

The first observation of a quantitative deficiency of I2 and I3 inner arms within flagella of *drc* mutants was obtained by the analyses of ^{35}S-labeled dynein heavy chains. The γ outer arm heavy chain and 1β inner arm heavy chain together were adopted as internal standards. Results from these analyses clearly indicated that flagella of some *drc* mutants contained low amounts of I2 and I3 inner arm heavy chains. The amounts of I2 and I3 inner arm heavy chains were 98%, in $sup_{pf}4$, and 57%, in *pf*3, of the amounts present in a wild-type strain. The mutants were ordered as follows depending on the I2 and I3 inner arm heavy chains loss: $sup_{pf}4 < sup_{pf}3 = pf2 < sup_{pf}5 < pf3$ (12). This evidence suggested to us that some of the *drc* proteins could form a binding site for I2 and I3 inner arms or be involved in a mechanism that makes I2 and I3 inner arms heavy chains competent to bind.

We considered that it was important to test these hypotheses because the outcome could help us to understand the pro-

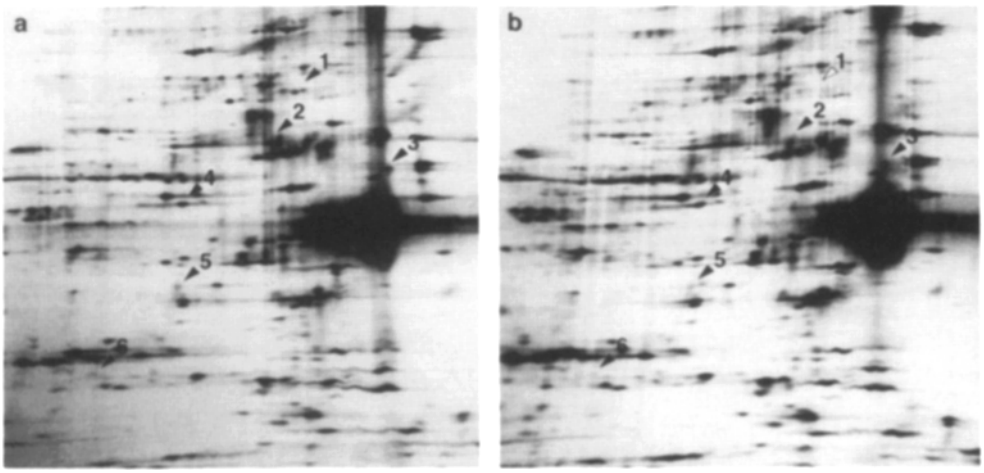

Figure 7. Autoradiograms of ^{35}S-labeled axonemal polypeptides that were resolved by two-dimensional electrophoresis. Only portions of the original maps resolving polypeptides in the 130,000–15,000 molecular weight range are shown. The gels are oriented with basic polypeptides on the left. Filled arrowheads and numbers indicate the *drc* components. (*a*) Axonemal components from $sup_{pf}5$ wild-type dikaryons. (*b*) Axonemal components from *pf*3 wild-type dikaryons. An empty arrowhead indicates the position of the *drc* component 1. That component is the putative defective gene product of *pf*3.

cess of flagellar assembly and function. Before testing the competence of axonemes from *drc* mutants to bind inner arm heavy chains in vitro we first intended to determine whether the I1 inner arms are lacking from flagella of *drc* mutants similarly to I2 and I3 inner arms.

This experiment had priority because our previous measurements of the amounts of I2 and I3 inner arm heavy chains were relative to the amounts of combined outer arms and I1 inner arm heavy chains. Therefore, they could be affected by a defect of I1 inner arms. Moreover, the observation that a *drc* defect affects also the binding of I1 inner arms to the axonemes could be relevant to explain the phenomenon of suppression of flagellar paralysis of radial spoke and central pair mutants.

Our inability to resolve the I1 inner arm heavy chains from the outer arm heavy chains prompted us to isolate *drc* recombinant strains carrying the *pf*28 mutation and consequently lacking the outer dynein arms. Through the recombinants we were able to measure the quantities of I1 inner arm heavy chains and found that I1 inner arms were defective similarly to I2 and I3 inner arms. Although this result was straightforward it lead us to the following consideration.

The presence in the same strain of two mutations affecting the binding of dynein arms to the axonemes resulted in the formation of flagella that were shorter than those of *pf*28 or each of the *drc* mutants (with the exception of sup_{pf}4*pf*28 flagella) (Table I). This evidence indicated that the absence of outer arms and part of inner arms have a negative and synergistic effect toward the assembly of flagella. Moreover, the amounts of I2 and I3 inner arms are lower in the recombinants than in the *drc* mutants (Table I of this article and Table IV of reference 12). These results suggested to us that together *pf*28 and *drc* mutations negatively affect inner arm binding to doublet microtubules. Nevertheless, we concluded that a defect of I1 inner arms in the recombinants likely is caused by the presence of the *drc* mutation because the I1 inner arm defect in *pf*3*pf*28 and sup_{pf}5*pf*28 is as extensive as that of I2 and I3 inner arms.

The molar ratio between the γ outer arm heavy chain and the 1β inner arm heavy chain is 4:1 (13) and the loss of 1β in sup_{pf}5*pf*28 is at the most 70%. Therefore, the internal standard adopted in our previous measurements of I2 and I3 inner arms in sup_{pf}5 could be 14% lower than in a wild-type strain. As a consequence it is possible that our assessment of I2 and I3 inner arm defect in sup_{pf}5 was underestimated. For the same reason other *drc* mutants also could be slightly more defective for I2 and I3 inner arms than previously reported (12).

The drc Components Alter the Binding of I2 and I3 Inner Arms to the Axonemes

We have measured the amounts of inner arms that bind in vitro to ATP-insensitive sites of dynein-depleted axonemes of wild-type and *drc* mutants. We found that the extraction of dynein arms increased the number of binding sites for inner arms as much as 11 times in a wild-type strain, whereas the absence of some *drc* components decreased the binding of I2 and I3 inner arms to approximately one third of the wild-type level. The concentration of rebound inner arms was reduced to an extent that depends on the *drc* defects. From these observations we deduced that the lattice of outer doublet microtubules does not bind I2 and I3 inner arms with high affinity, whereas the *drc* forms at least one type of inner arm binding site. The alternative that *drc* components modify and make I2 and I3 inner arm heavy chains competent to bind is unlikely because neither matrix proteins nor ATP are required for the binding.

A dual function of the *drc* in binding the inner arms and regulating their function is suggested by the behavior of the mutant sup_{pf}4. The mutant sup_{pf}4 is a suppressor of paralysis of radial spoke and central complex mutants like the rest of the *drc* mutants but is similar to a wild-type strain in inner arm content both in vivo and in vitro. As a consequence *drc* components 5 and 6, which are lacking from sup_{pf}4 as well as from other *drc* mutants, may be unnecessary for the inner arm binding but sufficient to cause flagellar paralysis in radial spoke or central pair mutants. Therefore, the *drc* may be formed by two parts: one regulating the function of I2 and I3 inner arms and the other binding the same arms to the A microtubule.

Among the *drc* components that form a putative binding site, components 1 and 2, which lack in *pf*3 and sup_{pf}5 axonemes, affect I2 and I3 inner arm binding in vivo more than components 3, 4 and 7, which lack in *pf*2. Components 1 and 2 of the *drc* may function as a complex that binds the inner arms, whereas components 3, 4 and 7 may increase the affinity of the binding site for the inner arms.

All parts of the *drc* may be located between the inner arms and the outer dynein arms, as was deduced from electron microscopy images of the mutant *pf*2 (10). We noticed that the lack of *drc* components 1, 2, 5, 6, and 7 and a protein mass of at least 378,000 is correlated with the lack of an electron-dense structure from the axoneme of *pf*2 that is touching both the I2 inner arm and one every four outer arms. From that location the *drc* may interact differently with each type of inner arm.

The *drc* also could coordinate the activity of both outer and inner arms within a 96-nm repeat along the doublet microtubules. The existence of such coordination is suggested by results of in vitro experiments. The movement of outer dynein arms in disintegrating axonemes generates a sliding velocity of doublet microtubules that is higher than that of inner dynein arms (8). However, in vivo both types of arms must move at a similar speed in order to work efficiently.

The Function of the drc In Vivo

The following evidence indicated that formation of asymmetric waveforms and therefore efficient swimming of *Chlamydomonas* require a flow of information passing from the central complex to the inner dynein arms through radial spokes and *drc*. First, axonemes deprived of central complex form symmetric waveforms after reactivation in vitro instead of the asymmetric waveforms that are formed by intact axonemes (5). Second, radial spoke mutants move the flagella with symmetric waveforms, if they also carry a mutation suppressing their paralysis (3). Third, the row of inner dynein arms must be complete in order to form the asymmetric waveforms of wild-type *Chlamydomonas* flagella (2). Finally, defects of the *drc* reduce the number of I2 and I3 inner arms bound to the axoneme (12).

Further evidence that the *drc* is a major part in the chain of structures linking the central complex to inner arms is described in this report. Defects of the *drc* affect the binding

of every type of inner arm to the axonemes in vivo and affect the ATP-insensitive binding of I2 and I3 inner arms to the axonemes in vitro. Therefore, the *drc* mediates the binding of inner arms to the lattice of the microtubule wall and regulates the functions of the same arms along and around the axoneme.

The fact that the same *drc* mutations reverse the paralyzing effects of either central complex or radial spoke mutations reinforces the evidence that there is a flow of information passing through the central complex, the radial spokes, the *drc* and, finally, the dynein arms.

Signals passing from the central complex to the dynein arms do not require necessarily a physical contact. For instance, the I1 inner arm mutant *pf*9-2 was obtained as a bypass suppressor of the temperature-sensitive central complex mutant *pf*16BR3. However, it does not suppress the paralyzed flagella phenotype of other central complex or radial spoke mutations (15). Therefore, the interaction between the *pf*9-2 and *pf*16BR3 mutations represent a specific interaction between the central complex and the I1 inner arms and not a more general bypass mechanism such as that shown by all other mutations suppressing flagellar paralysis of central complex and radial spoke mutants.

Perspectives

Our study of inner arm binding through quantitative analyses of I2 and I3 inner arm bound in vitro extends previous observations indicating that inner arms must rebind to axonemal doublet microtubules at specific sites (17). We have focused on the ATP-insensitive binding sites of inner arms and identified the *drc* as the adapter that binds I2 and I3 inner arms. The fact that inner arm reconstitution on the outer doublets also restores the ability of the axoneme to disintegrate (17) will allow us to determine whether the absence of *drc* components alters the sliding velocity of microtubules.

This work was supported by the grant GM-44467 from the National Institutes of Health.

Received for publication 22 November 1993 and in revised form 7 February 1994.

References

1. Adams, G. M., B. Huang, G. Piperno, and D. J. Luck. 1981. Central-pair microtubular complex of *Chlamydomonas* flagella: polypeptide composition as revealed by analysis of mutants. *J. Cell Biol.* 91:69–76.
2. Brokaw, C. J., and R. Kamiya. 1987. Bending patterns of *Chlamydomonas* flagella: IV. Mutants with defects in inner and outer dynein arms indicate differences in dynein arm function. *Cell Motil. Cytoskeleton.* 8:68–75.
3. Brokaw, C. J., D. J. Luck, and B. Huang. 1982. Analysis of the movement of *Chlamydomonas* flagella: the function of the radial-spoke system is revealed by comparison of wild-type and mutant flagella. *J. Cell Biol.* 92:722–732.
4. Ebersold, W. T., and R. P. Levine. 1959. A genetic analysis of linkage group I of *Chlamydomonas reinhardtii*. *Z. Vererbungsl.* 90:74–82.
5. Hosokawa, Y., and T. Miki-Noumura. 1987. Bending motion of *Chlamydomonas* axonemes after extrusion of central-microtubules. *J. Cell Biol.* 105:1297–1301.
6. Huang, B., G. Piperno, Z. Ramanis, and D. J. Luck. 1981. Radial spokes of *Chlamydomonas* flagella: genetic analysis of assembly and function. *J. Cell Biol.* 88:80–88.
7. Huang, B., Z. Ramanis, and D. J. Luck. 1982. Suppressor mutations in *Chlamydomonas* reveal a regulatory mechanism for flagellar function. *Cell.* 28:115–124.
8. Kurimoto, E., and R. Kamiya. 1991. Microtubule sliding in flagellar axonemes of Chlamydomonas mutants missing inner- or outer-arm dynein: velocity measurements on new types of mutants by an improved method. *Cell Motil. Cytoskeleton.* 19:275–81.
9. Luck, D., G. Piperno, Z. Ramanis, and B. Huang. 1977. Flagellar mutants of *Chlamydomonas*: studies of radial spoke-defective strains by dikaryon and revertant analysis. *Proc. Natl. Acad. Sci. USA.* 74:3456–3460.
10. Mastronarde, D. N., E. T. O'Toole, K. L. McDonald, J. R. McIntosh, and M. E. Porter. 1992. Arrangement of inner dynein arms in wild-type and mutant flagella of *Chlamydomonas*. *J. Cell Biol.* 118:1145–1162.
11. Mitchell, D. R., and J. L. Rosenbaum. 1985. A motile *Chlamydomonas* flagellar mutant that lacks outer dynein arms. *J. Cell Biol.* 100: 1228–1234.
12. Piperno, G., K. Mead, and W. Shestak. 1992. The inner dynein arms I2 interact with a "dynein regulatory complex" in *Chlamydomonas* flagella. *J. Cell Biol.* 118:1455–1463.
13. Piperno, G., and Z. Ramanis. 1991. The proximal portion of *Chlamydomonas* flagella contains a distinct set of inner dynein arms. *J. Cell Biol.* 112:701–709.
14. Piperno, G., Z. Ramanis, E. F. Smith, and W. S. Sale. 1990. Three distinct inner dynein arms in *Chlamydomonas* flagella: molecular composition and location in the axoneme. *J. Cell Biol.* 110:379–389.
15. Porter, M. E., J. Power, and S. K. Dutcher. 1992. Extragenic suppressors of paralyzed flagellar mutations in Chlamydomonas reinhardtii identify loci that alter the inner dynein arms. *J. Cell Biol.* 118:1163–76.
16. Sager, R., and S. Granick. 1953. Nutritional studies with *Chlamydomonas reinhardtii*. *Ann. NY Acad. Sci.* 466:18–30.
17. Smith, E. F., and W. S. Sale. 1992. Structural and functional reconstitution of inner dynein arms in *Chlamydomonas* flagellar axonemes. *J. Cell Biol.* 117:573–581.
18. Witman, G. B. 1986. Isolation of *Chlamydomonas* flagella and flagellar axonemes. *In* Methods in Enzymology. Vol. 134. R. B. Vallee, editor. Academic Press, Inc., Orlando, FL. 280–290.